We are IntechOpen, the world's leading publisher of Open Access books Built by scientists, for scientists

4,800
Open access books available

122,000
International authors and editors

135M
Downloads

Our authors are among the

154
Countries delivered to

TOP 1%
most cited scientists

12.2%
Contributors from top 500 universities

CLARIVATE ANALYTICS BOOK CITATION INDEX INDEXED

WEB OF SCIENCE™

Selection of our books indexed in the Book Citation Index in Web of Science™ Core Collection (BKCI)

Interested in publishing with us?
Contact book.department@intechopen.com

Numbers displayed above are based on latest data collected.
For more information visit www.intechopen.com

12

Sound Waves Generated Due to the Absorption of a Pulsed Electron Beam

A. Pushkarev, J. Isakova, G. Kholodnaya and R. Sazonov
Tomsk Polytechnic University
Russia

1. Introduction

Over the past 30–40 years, a large amount of research has been devoted to gas-phase chemical processes in low-temperature plasmas. When the low-temperature plasma is formed by a pulsed electron beam, there is a significant reduction, compared to many other methods of formation, in the power consumption for conversion of gas-phase compounds. Analysis of experimental studies devoted to the decomposition of impurities of various compounds (NO, NO_2, SO_2, CO, CS_2, etc.) in air by a pulsed electron beam showed (Pushkarev et al., 2006) that the the energy of the electron beam required to decompose one gas molecule is lower than its dissociation energy. This is due to the fact that under the action of the beam, favourable conditions for the occurrence of chain processes are formed. At low temperatures, when the initiation of a thermal reaction does not occur, under the influence of the plasma there are active centres—free radicals, ions or excited molecules, which can start a chain reaction. This chain reaction will take place at a temperature 150–200 degrees lower than a normal thermal process, but with the same speed. The impact of the plasma facilitates the most energy intensive stage, which is the thermal initiation of the reaction. A sufficient length of the chain reaction makes it possible to reduce the total energy consumption for the chemical process. The main source of energy in this case is the initial thermal energy or the energy of the exothermic chemical reactions of the chain process (e. g., oxidation or polymerization). It is important to note that when conducting a chemical process at a temperature below the equilibrium, one may synthesize compounds which are unstable at higher temperatures or for which the selectivity of the synthesis is low at higher temperatures. For efficient monitoring of the chemical processes, optical techniques are used (emission and absorption spectroscopy, Rayleigh scattering, etc.), chromatography and mass spectrometry (Zhivotov et al., 1985) which all require sophisticated equipment and optical access to the reaction zone.

When the energy of a pulsed excitation source (spark discharge, pulsed microwave discharge, pulsed high-current electron beam, etc.) is dissipated in a closed plasma reactor, then, as a result of the radiation-acoustic effect (Lyamshev, 1996), acoustic oscillations are formed due to the heterogeneity of the excitation (and, thereafter, heating) of the reagent gas. The measurement of sound waves does not require the use of sophisticated equipment, which give a lot of information about the processes occurring in the plasma reactor (Pushkarev et al., 2002; Remnev et al., 2001; Remnev et al., 2003a).

2. Experimental installation

This paper presents the results of the study of sound waves generated in gas mixtures when the energy dissipation of a pulsed high-current electron beam in a closed plasma reactor occurs. The scheme of measurements is shown in Fig. 1.

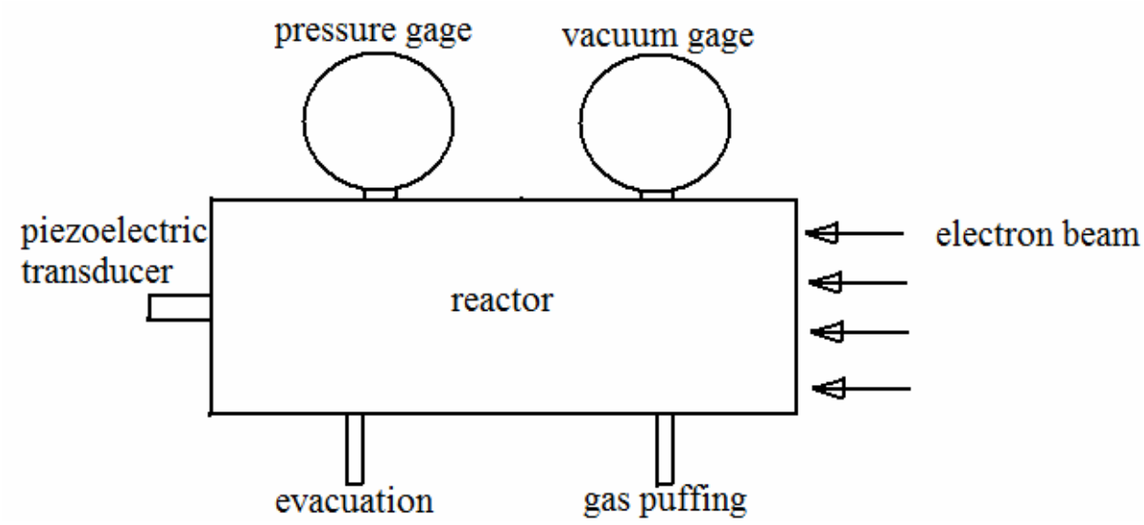

Fig. 1. Experimental scheme

The signal from a piezoelectric transducer was recorded using an oscilloscope Tektronix 3052B (500 MHz, $5 \cdot 10^9$ measurements/s). The source of the high-current electron beam is the accelerator TEA-500 (Remnev et al., 2004a, 2004b). Fig. 2 shows an external view of the TEA-500 accelerator.
In Fig. 3, typical oscilloscope traces of voltage and total electron beam current are shown.

Fig. 2. The TEA-500 accelerator

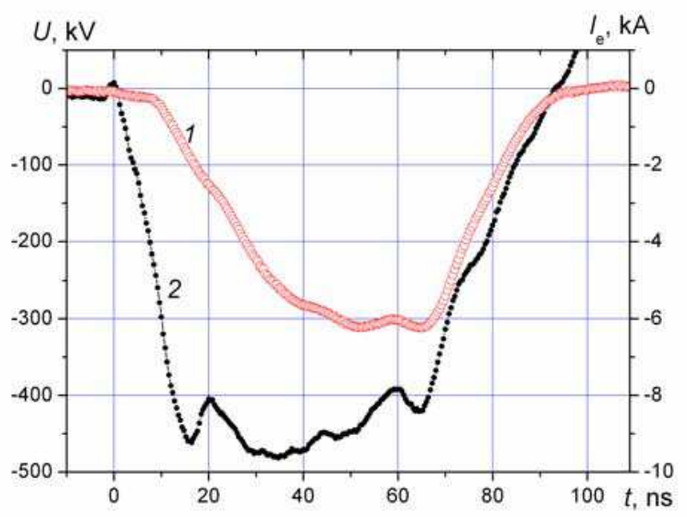

Fig. 3. Oscilloscope traces of electron current (1) and accelerating voltage (2)

These graphs are averaged for 10 pulses with a frequency of 1 impulse/s after operating the cathode for 10–20 pulses. The parameters of the electron beam are given in Table 1.

Electron energy	450–500 keV
Ejected electron current	up to 12 kA
Half-height pulse duration	80 ns
Pulse repetition rate	up to 5 pulses/s
Pulse energy	up to 200 J

Table 1. Parameters of the high-current pulsed electron beam

In Fig. 4 the spatial distribution of the energy density of the electron beam formed by the diode with a cathode made from a carbon fibre is illustrated.

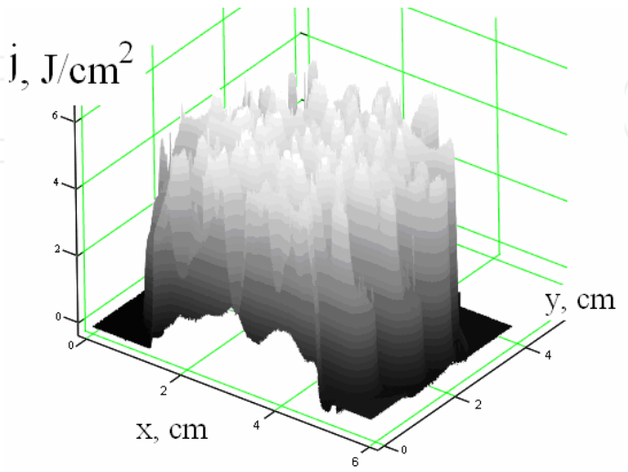

Fig. 4**.** The spatial distribution of the energy density of a pulsed electron beam

Most of the experiments were carried out with the reactor, comprised of a cylinder of quartz glass with an inner diameter of 14.5 cm and a volume of 6 litres. It is constructed in a tubular form; the electron injection begins from the titanium foil at the end of the tube. At the output flange of the plasma reactor there are a number of tubes used to connect a vacuum gauge and a manometer, a piezoelectric transducer, for an initial injection of the reagent mixture and for the evacuation of the reactor before a gas pumping. Other reactors, with a diameter of 6 cm and a length of 11.5 cm, with a diameter 9 cm and a length of 30 cm, were used as well. Fig. 5 shows a photograph of the plasma chemical reactor.

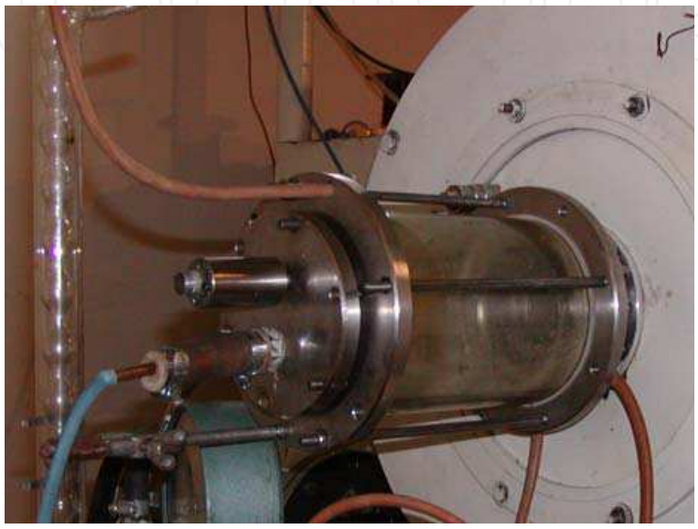

Fig. 5. Plasma chemical reactor with a volume of 6 litres

The sound waves were recorded by a piezoelectric transducer. Throughout the study, gas mixtures of argon, nitrogen, oxygen, methane, silicon tetrachloride and tungsten hexafluoride were used. When measuring pressure in the reactor using the piezoelectric transducer, we recorded the standing sound waves. An electrical signal coming from the piezoelectric transducer does not require any additional amplification. A typical oscilloscope trace of the signal is shown in Fig. 6. The reactor length is 39 cm and its inner diameter is 14.5 cm.

Test measurements were performed on an inert gas (Ar, 1 atm) to avoid any contribution of chemical transformations under the influence of the electron beam at a change in frequency of sound waves. For further signal processing it was necessary to transform it into digital form. In Fig. 7, a spectrum obtained by Fourier transformation of the signal shown in Fig. 6 is presented.

In our experimental conditions, the precision of measurement of the frequency is ±1.5 Hz.

3. Investigations of the frequency of the sound waves

In a closed reactor with rigid walls, after the dissipation of a pulsed electron beam, whose frequency for an ideal gas is equal to (Isakovich, 1973):

$$f_n = \frac{n}{2 \cdot l}\sqrt{\frac{\gamma R T}{\mu}} \quad , \tag{1}$$

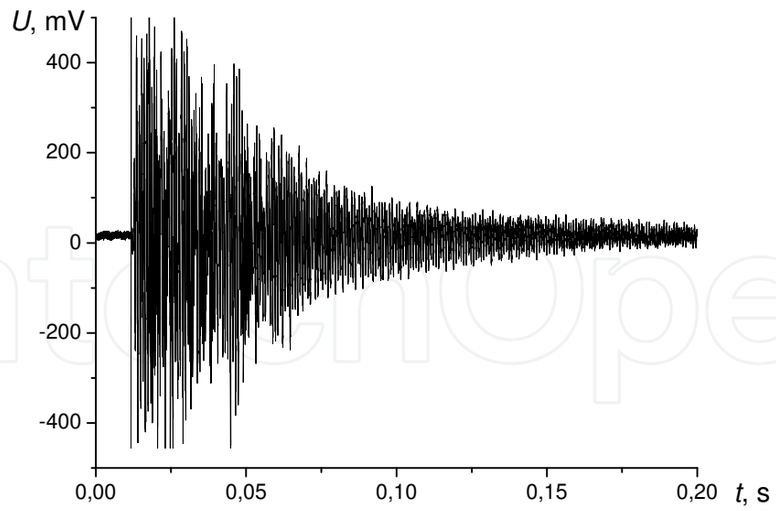

Fig. 6. Signal from the piezoelectric transducer

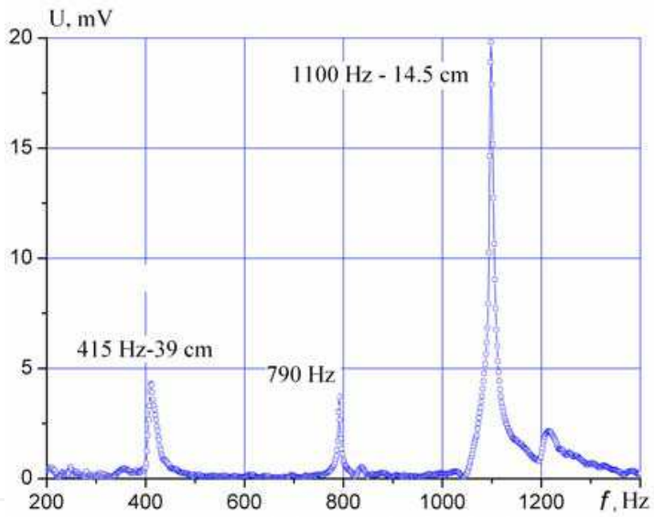

Fig. 7. The frequency spectrum of the signal from piezoelectric transducer. 415 Hz corresponds to the longitudinal sound waves, 1100 Hz is for transverse sound waves

where n is the harmonic number (n = 1, 2, ...), l is the length of the reactor, γ is the adiabatic exponent, R is the universal gas constant, and T and μ are, respectively, the temperature and molar mass of the gas in the reactor.

In the experiments we recorded the sound vibrations that correspond to the formation of standing waves along the reactor and across. For this study, the low-frequency component of the sound waves corresponding to the fundamental frequency (n = 1) waves propagating along the reactor was chosen.

The dependence of the frequency of the sound waves in the plasma reactor on the parameter $(\gamma/\mu)^{0.5}$ for different single-component gases is shown in Fig. 8 for the reactor with a length of 11.5 and 30 cm. The figure shows that in the explored range of frequencies the sound vibrations are well described by the relation for the ideal gases.

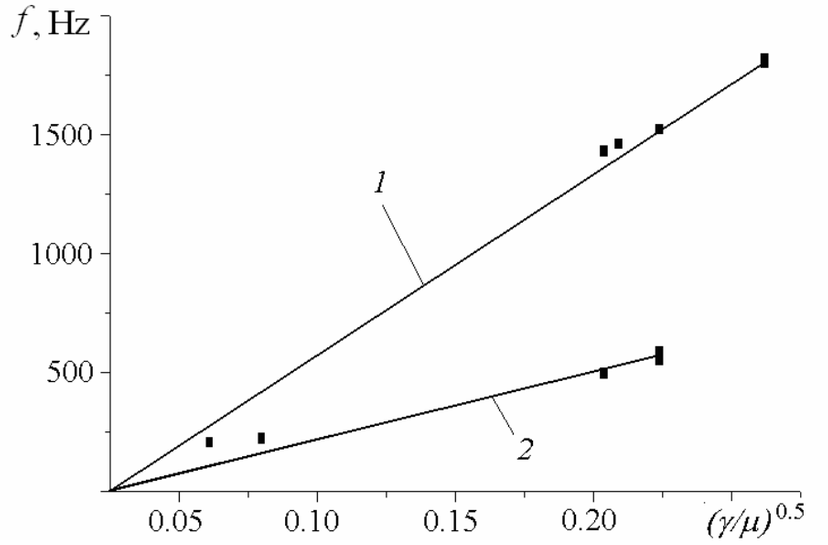

Fig. 8. The dependence of the frequency of the sound vibrations in the reactor on the ratio of the adiabatic exponent to the molar mass of single-component gases. Dots correspond to experimental data, lines are the calculations by (Eq.1) at l = 11.5 cm (1) and 30 cm (2).

In real plasma chemical reactions, multicomponent gas mixtures are used and the reaction products also contain a mixture of gases. When calculating the frequency of acoustic oscillations a weighting coefficient of each component of the gas mixture should be taken into account and the calculation should be performed using the following formula (Yaworski and Detlaf, 1968):

$$f_{sound} = \frac{\sqrt{RT}}{2l\sqrt{m_0}} \sqrt{\sum_i \frac{\gamma_i m_i}{\mu_i}}\,, \tag{2}$$

where m_0 is the total mass of all components of the gas mixture; and m_i, γ_i, μ_i are, respectively, the mass, adiabatic exponent and molar mass of the i-th component.
Given that the mass of the i-th component is equal to

$$m_i = 1.66 \cdot 10^{-27} \mu_i N_i = K \mu_i \frac{P_i V}{P_0}\,,$$

where N_i is the number of molecules of i-th component, P_i is its partial pressure, V is the reactor volume, P_0=760 Torr, and K is a constant.
Then (2) can be written in a more convenient way:

$$f_{sound} = \frac{\sqrt{RT}\sqrt{\sum_i \gamma_i P_i}}{2l\sqrt{\sum_i \mu_i P_i}}\,. \tag{3}$$

Fig. 9 shows the dependence of the frequency of sound vibrations, resulting in a plasma chemical reactor when an electron beam is injected into two- and three-component mixtures, on the parameter φ defined by

$$\varphi = \frac{\sqrt{\sum_i \gamma_i P_i}}{\sqrt{\sum_i \mu_i P_i}}.$$

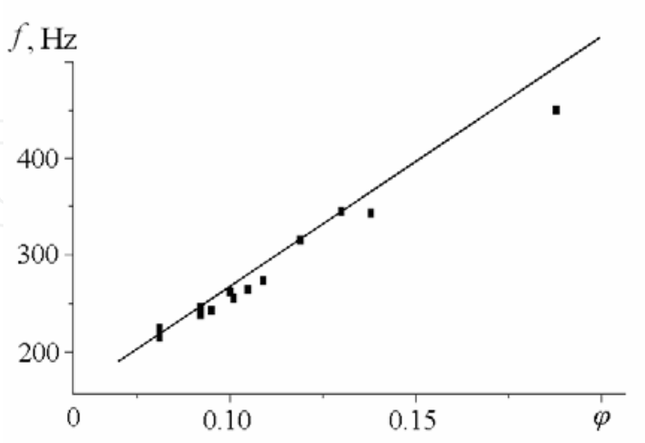

Fig. 9. The dependence of the frequency of sound oscillations in the plasma chemical reactor with a length of 30 cm on the parameter φ for gas mixtures. The points correspond to the experimental values, the lines are calculated from (3).

The frequency measurements of sound vibrations which arise in the plasma chemical reactor from the injection of pulsed electron beams into two- and three-component mixtures, showed that the calculation using (3) leads to a divergence between the calculated and experimental values of under 10%, and at frequencies below 400 Hz, less than 5%.

From (2) and (3) it is observed that the frequency of the sound waves depends on the gas temperature in the reactor, so the temperature should also be monitored. Let us determine the measurement accuracy which is necessary to measure the temperature so that the measurement error of the conversion level does not exceed the error due to the limitations in the accuracy of the frequency measurement. For transverse sound waves in argon (γ = 1.4, μ = 40, l = 0.145 m), (2) gives us that $f_{sound} = 64.2 \cdot (T)^{0.5}$.

This dependence is shown in Fig. 10.

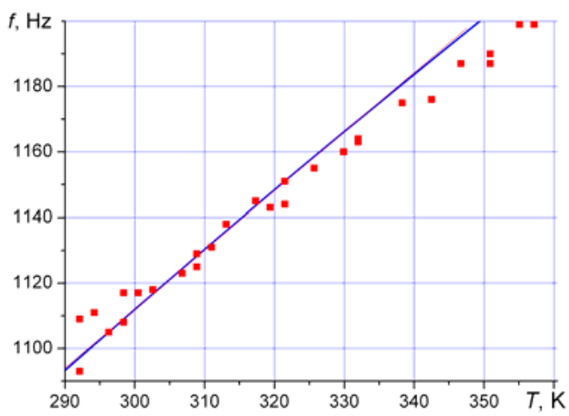

Fig. 10. The dependence of the frequency of transverse sound waves on the gas temperature. The points correspond to the experimental values, the lines - calculation by (2).

The calculated dependence of the frequency of transverse waves on temperature for the range 300–350 K is approximated by the formula f_{calc} = 570+1.8T. It follows that if the accuracy of measuring the frequency of the sound waves is 1.5 Hz it is necessary to control the gas temperature with an accuracy of 0.8 degrees. When measuring the spectrum of sound waves in the reactor, which has different temperatures over its volume, the profile of the spectrum is expanding. But it does not interfere with determining the central frequency for a given harmonic.

4. Investigation of the energy of sound waves

In a closed plasma chemical reactor when an electron beam is injected, standing waves are generated whose shape in our case is close to being harmonic. Then the energy of these sound waves is described by (Isakovich, 1973):

$$E = 0.25\,\beta\,\Delta P_s V \tag{4}$$

where β is the medium compressibility, ΔP_s is the sound wave amplitude, and V is the reactor volume.

At low compression rates (ΔP_s <<1) and if the momentum conservation law is implemented (under damping), the medium compressibility can be calculated by the formula (Isakovich, 1973):

$$\beta = \left(\rho C_s^2\right)^{-1}, \tag{5}$$

where ρ is the density of the gas and C_s is the velocity of sound in the gas.

Fig. 11 shows the change in pressure in the reactor after the injection of the beam (Pushkarev et al., 2001).

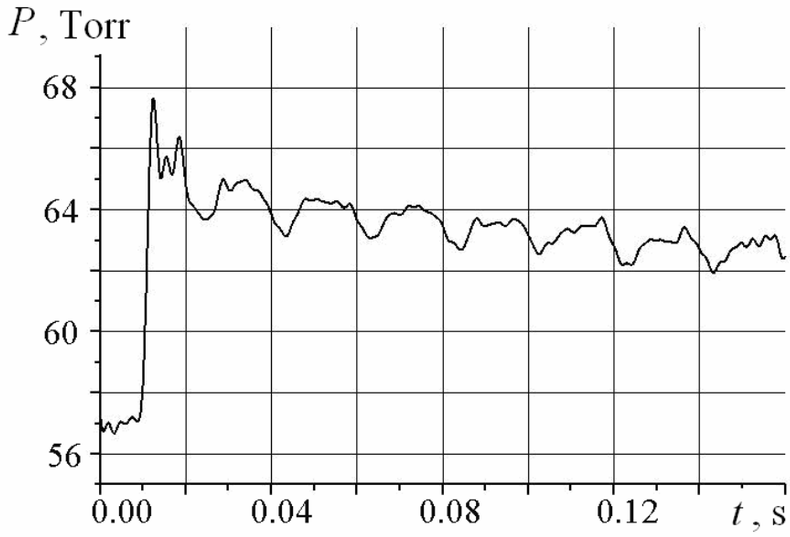

Fig. 11. The change of pressure in the reactor filled with a mixture of hydrogen and oxygen, after the injection of a pulsed electron beam in an absence of combustion.

It is evident that a decrease in pressure in the reactor (due to cooling of the gas), after a sharp increase is sufficiently slow and hence the speed of response of the pressure sensor is adequate for recording a complete change of pressure in the reactor. The dependence of the energy of the sound vibrations in the reactor on the electron beam energy, which is absorbed in the gas, is shown in Fig. 12.

The electron beam energy absorbed by the gas was calculated as the product of the heat capacity of the gas and the mass and the change in the gas temperature. The change of the gas temperature in a closed reactor was determined from the equation of the ideal gas state regarding a change in pressure. Pressure changes were recorded with the help of a fast pressure sensor SDET-22T-B2. The energy of the sound waves was about 0.2% of the electron beam energy absorbed in the gas.

For nitrogen and argon in a wide pressure range (and thus of energy input of the beam into the gas), a good correlation between the energy of sound vibrations and the energy input of the beam into a gas was obtained, which allows evaluation of the energy input of the beam into a gas using the amplitude of the sound waves.

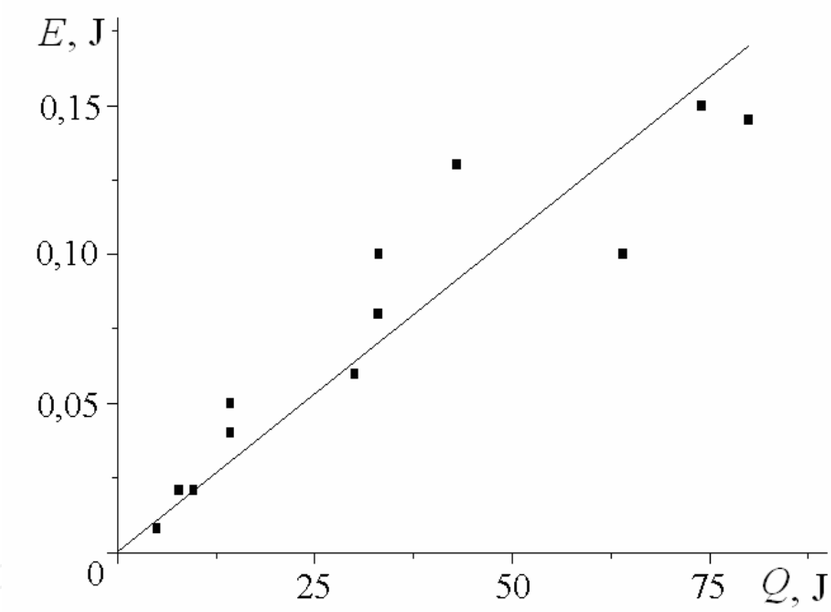

Fig. 12. Dependence of the energy of the sound vibrations in the reactor on the energy of the electron beam absorbed in the gas. The points correspond to the experimental values, the line is an approximation by a polynomial of the first order

5. Investigation of the acoustic attenuation

The presence of gas particles whose size is much larger than the gas molecules causes an increase in the attenuation of sound waves propagating in a gas. You can observe such an effect when watching the attenuation of sound in fog. Sound propagation in the suspensions of microparticles in the gas was studied in (Molevich and Nenashev, 2000) when propagating in open space. To control the process of formation of particles in a volume of the reactor to measure an attenuation of acoustic vibrations is needed, but it is necessary to

estimate the sound attenuation in the reactor in the case of absence of microparticles, or aerosol.
Since the waveform of sound oscillations generated in the reactor during the injection of high-current electron beam is close to being harmonic, then a change of energy of the sound waves due to absorption is as follows (Isakovich, 1973):

$$E(t) = E_0\, e^{-\alpha t},$$

where α is the time coefficient of absorption.
When the sound waves are propagating in a tube closed from both sides, the absorption coefficient is (Isakovich, 1973):

$$a = a_1 + a_2 + a_3 + a_4$$

where α_1 is the sound absorption coefficient when propagating in an unbounded gas, α_2 is the sound absorption coefficient for reflection from the side walls of the pipe when propagation along the pipe, α_3 is the absorption coefficient when reflection is on the ends of the pipe, and α_4 is the absorption coefficient due to friction on the pipe wall.

5.1 The absorption coefficient of sound when propagating in an unbounded gas

The absorption coefficient of sound wave energy in a gas due to thermal conduction and the shear viscosity of a gas can be calculated by the Stokes–Kirchhoff formula (Isakovich, 1973):

$$\alpha_1 = \frac{(2\pi f_{sound})^2}{2\rho C_{sound}^2}\left[\frac{4}{3}\eta + \chi\left(\frac{1}{C_v} - \frac{1}{C_p}\right)\right], \tag{6}$$

where η is the shear-viscosity coefficient (g/cm·s), χ is the heat conductivity coefficient (cal/cm·s·deg), and C_v and C_p are, respectively, the heat capacity of the gas when the volume is constant, and when the pressure is constant (cal/g·deg).

5.2 The absorption coefficient when reflected from the side walls of the pipe

For a low-frequency sound wave which is propagating through a circular pipe, provided that $\lambda > 1.7d$ (where λ is the wavelength and d is the pipe diameter) the wave front is flat and the damping coefficient of the energy of sound wave when it is propagating along the pipe with ideal thermally conductive walls can be calculated by Kirchhoff's formula (Konstantinov, 1974):

$$\alpha_2 = \frac{1}{r_0}\sqrt{\frac{\pi f_s}{\rho}}\left[(\gamma - 1)\sqrt{\frac{\chi}{\gamma C_p}} + \sqrt{\eta}\right],$$

where r_0 is the pipe radius.
Taking into account that $\rho = \rho_0 P/P_0$, where P is the gas pressure in reactor and ρ_0 is the density of gas at normal conditions, P_0=760 Torr, then:

$$\alpha_2 = \frac{K_1}{r_0}\sqrt{\frac{f_s}{P}} \quad , \; K_1 = \sqrt{\frac{\pi P_0}{\rho_0}}\left[(\gamma - 1)\sqrt{\frac{\chi}{\gamma C_p}} + \sqrt{\eta}\right] \quad . \tag{7}$$

5.3 The absorption coefficient of sound when reflected from the ends of the pipe

The energy of sound waves reflected from the wall is

$$E = E_0(1\text{-}\delta),$$

where δ is the coefficient of energy absorption of sound wave for a single reflection and E_0 is the energy of the incident wave.
After n reflections $E_n = E_0(1\text{-}\delta)^{\text{-n}}$. After n reflections during the time t a sound wave will pass the distance $L = n \cdot l = C_s \cdot t$, therefore it can be written

$$n = \frac{C_s\, t}{l}$$

Then the change in the energy of sound waves reflected at the ends of a pipe is

$$E(t) = E_0(1-\delta)^{-\frac{C_s\, t}{l}} \tag{8}$$

If the change in energy of sound waves when reflected at the ends of the pipe is written as

$$E(t) = E_0 e^{-\alpha_3\, t} \tag{9}$$

then from (8) and (9) we obtain

$$\alpha_3 = \frac{C_s \ln(1-\delta)}{l} \tag{10}$$

Under the normal incidence of a flat wave on a metal wall, which is a good heat conductor, the absorption coefficient of sound wave energy is (Molevich and Nenashev, 2000):

$$\delta = 4(\gamma - 1)\sqrt{\frac{\pi f_s \chi}{\gamma C_p P}} \quad . \tag{11}$$

But if we consider only a normal incidence of a sound wave onto the ends of the reactor, we would neglect the absorption of sound waves reflected from the side walls of the reactor (i.e., $\alpha_2 = 0$). The absorption of sound at the same time will be forced by the thermal conductivity and viscosity of the gas and by absorption when reflected from the ends of the reactor, as in (6) and (10). As will be shown below, the experimentally measured absorption coefficients of the sound wave energy in the reactor is several times higher than the values which are calculated by (6) and (10). Therefore, when there is a reflection from the ends of the reactor, the dependence of the absorption coefficient on the angle of the incidence should be taken into account and the calculation should be performed by the formula (Molevich Nenashev, 2000):

$$\delta = \sqrt{\frac{f_s}{\gamma P}}\left[0.39(\gamma - 1)\sqrt{\frac{\chi}{C_p}} + 0.37\sqrt{\eta}\right], \tag{12}$$

From (10) and (12) we obtain (noting that when δ<<1, the quantity ln(1-δ)≈δ):

$$\alpha_3 = \frac{K_2}{l}\sqrt{\frac{f_s}{P}}, \text{ where } K_2 = C_s\left[0.39(\gamma-1)\sqrt{\frac{\chi}{\gamma C_p}} + 0.37\sqrt{\frac{\eta}{\gamma}}\right], \tag{13}$$

To take into account the energy losses of the sound wave due to friction on the wall is important in cases where the diameter of the pipe is comparable to the mean free path of gas molecules, i.e. for capillaries. In our case, it can be assumed that $\alpha_4 \approx 0$.

5.4 Calculation of the total absorption coefficient

Then the total absorption coefficient of sound wave energy in a closed reactor can be written as (Pushkarev, 2002):

$$\alpha = \left(\frac{K_1}{r_0} + \frac{K_2}{l}\right)\sqrt{\frac{f_s}{P}}, \tag{14}$$

where K_1 and K_2 are calculated by the (7) and (13), r_0 and l are taken in cm, f_s is in Hz, and P is in Torr. The coefficients K_1 and K_2 for the investigated gases are summarized in Table 2.

gas	K_1	K_2
N_2	25	218
O_2	27	189
Ar	32	254
WF_6	6.5	52
$SiCl_4$	5.9	45.7

Table 2. Calculated damping coefficients

Numerical estimates of the contribution of the different mechanisms of absorption of the sound waves in the reactor show that the influence of volume absorption (due to the thermal conductivity and viscosity of the gas) is insignificant. For the sound waves which are generated in the reactor 30 cm long, filled with nitrogen, at a pressure of 500 Torr: $\alpha_1=1.8\cdot10^{-3}$ s^{-1}, $\alpha_2=5.9$ s^{-1} , $\alpha_3=7.7$ s^{-1}. The total absorption coefficient, which takes into account only the normal incidence of sound-sound wave (i.e., $\alpha_2=0$, $\alpha_3=1.2$ s^{-1}) is much smaller than the experimentally measured coefficient for these conditions (14.7 s^{-1}). It is important to note that when the sound waves are propagating in a closed reactor the main contribution (60%–80%) to the absorption is made by the viscosity of the gas. The magnitude of the second term in (7) and (13) is more than the first term by 3–9 times (for different gases). The contribution of the side walls of the reactor and its ends to the absorption of sound waves is approximately the same for a large reactor. The ratio of energy absorption of sound waves in the reactor for different harmonics is shown in Fig. 13.

An electron beam was injected into the 30 cm long reactor, filled with argon at different pressures. To compare the attenuation coefficients in the different plasma-chemical reactors (lengths 11.5 and 30 cm) and in different gases, the value of the attenuation coefficient was normalized by the coefficient K:

$$K = \left(\frac{K_1}{r_0} + \frac{K_2}{l} \right),$$

Fig. 13 shows that the magnitude of the absorption coefficient is proportional to the square root of frequency of sound waves, in accordance with the (14).

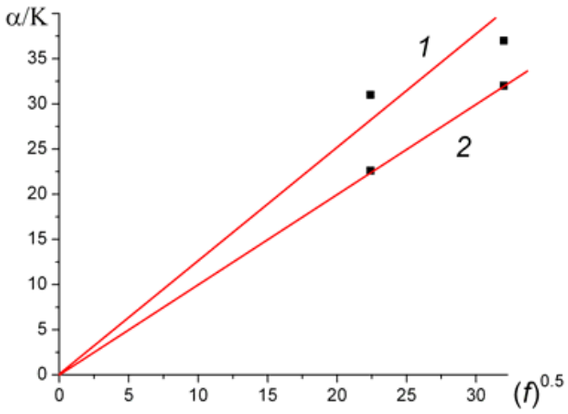

Fig. 13. The dependence of the absorption coefficient of energy of sound waves in the reactor on f_s. The points correspond to the experimental values, lines, to calculation by (14). The gas is argon, 1–400 Torr and 2–500 Torr.

6. Analysis of the conversion level of gas-phase compounds with respect to a change of sound wave frequency

By simple calculations, it can be shown that for a chemical reaction in which both the initial mixture of reagents and the mixture after the reaction are a gas (no phase transition), then the frequency of sound vibrations after the reaction, is equal to that in the initial mixture. A slight change in frequency of standing sound waves can be associated only with changes in the adiabatic exponent. But if a reaction produces solid or liquid products, the frequency of the sound waves will vary. For the pyrolysis reaction of methane:

$$CH_4 = 2H_2 + C$$

The decrease of methane on the value of ΔP will lead to the formation of $P_i = 2\Delta P$ of hydrogen. Let us denote the methane conversion level as $\alpha = \Delta P/P_0$. Then from (3) we obtain:

$$f_s = \frac{\sqrt{RT} \cdot \sqrt{\gamma_1(1-\alpha) + 2\gamma_2\alpha}}{2l \cdot \sqrt{\mu_1(1-\alpha) + 2\mu_2\alpha}}, \tag{15}$$

where γ_1 and μ_1 are, respectively, the adiabatic index and molar mass of methane, and γ_2 and μ_2 are, respectively, the adiabatic index and molar mass of hydrogen.

For the reactor with an inner diameter of 14.5 cm, the dependence of the level of methane conversion on the frequency of the transverse sound waves is shown in Fig. 14.

When the measurement accuracy of the sound waves frequency is 1.5 Hz and the accuracy of the temperature is 0.8 degrees, the developed method allows controlling the level of conversion of methane to carbon with an accuracy within 0.1% (Pushkarev et al., 2008). A

weak damping of sound waves makes possible to measure the oscillation frequency with a fine resolution.
When measuring the frequency of sound waves in a reactor filled with methane, the frequency spectrum obtained is shown in Fig. 15.

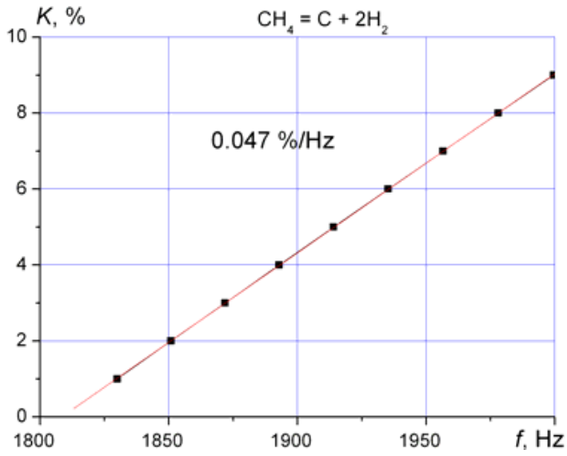

Fig. 14. Dependence of the conversion level of methane in the pyrolysis reaction on the frequency of transverse sound waves.

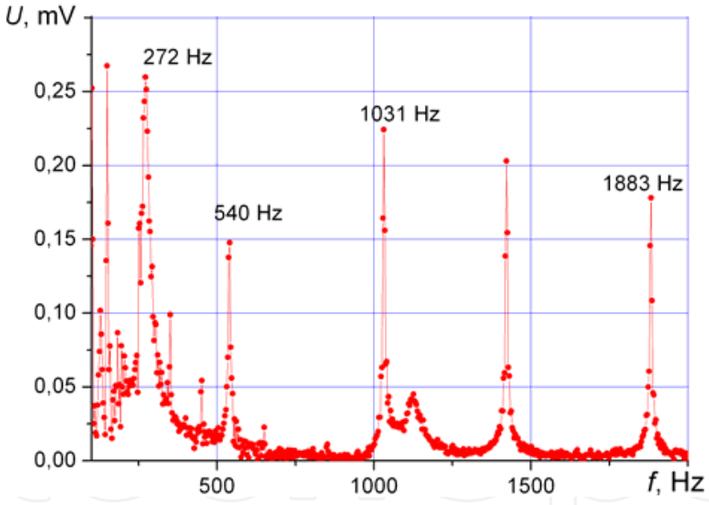

Fig. 15. The spectrum of sound waves in a reactor filled with methane after injection of high-current electron beam.

In Fig. 16, the frequency spectrum in the range of higher harmonics is shown.
In Fig. 17 the dynamics of methane conversion under the influence of a pulsed electron beam is shown.
Adding argon causes an increase in the error in determinating the level of conversion. In the reaction:

$$CH_4 + \beta \cdot Ar = CH_4 \cdot (1-\alpha) + 2\alpha \cdot H_2 + \beta \cdot Ar + \alpha \cdot C$$

where a is the conversion level of methane and β is the contents of argon in a mixture.

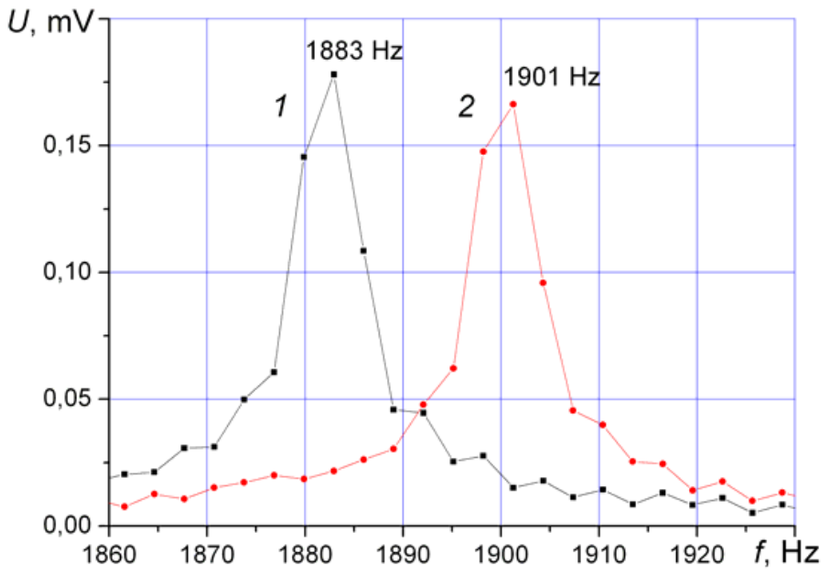

Fig. 16. The spectrum of sound waves in methane: initially (1), and after irradiation by 500 pulses: (2).

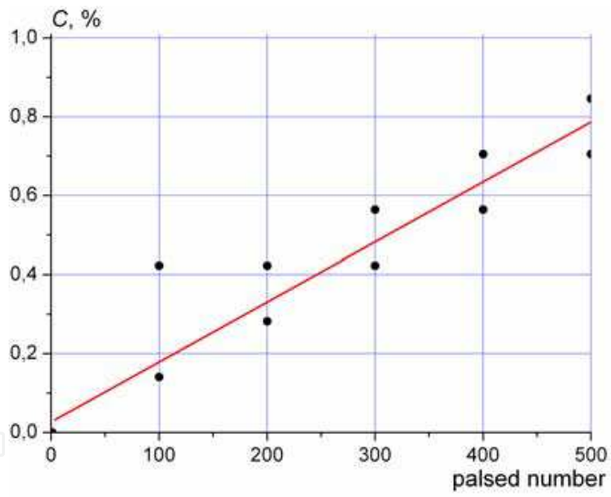

Fig. 17. The dependence of the conversion level of methane pyrolysis on the number of pulses in the electron beam.

In Fig. 18 the dependence of the error in determining the level of conversion of methane (in the pyrolysis reaction) on the percentage content of argon in a mixture of methane and argon is shown. The content of argon was calculated in relation to the volume of methane. 50% argon corresponds to 33% of the total volume of the mixture in the reactor.

The technique developed is designed for operational control of the technology process and can also be used to control the processes of recovery of halogenides of various compounds (Remnev et al., 2004c). Fluoride compounds are widely used in the production of rare earth metals and isotopic enrichment. When restoring halogenides, compounds with a high chemical activity (F_2, HF, HCl, etc.) are formed. Registration of the sound waves does not

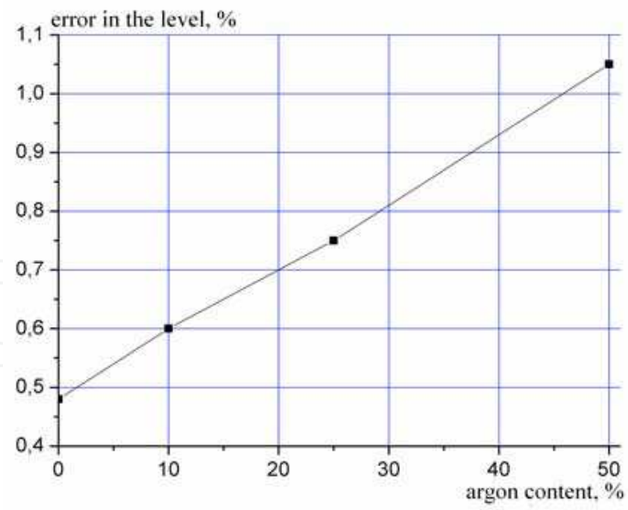

Fig. 18. Dependence of error in determining the level of conversion of methane mixed with argon on the argon content.

require access to the reaction zone, which prevents the destruction of diagnostic equipment. Measurements of the frequency of sound vibrations generated during the dissipation of energy of a pulsed excitation source, make it possible to control the progress of a plasma chemical reaction in the formation of solid products, such as the reaction of $CO_2 \rightarrow C+O_2$; $WF_6 \rightarrow W+3F_2$, etc.

This method gives the average degree of conversion over the reactor volume, which is of particular advantage in avoiding the errors associated with the localization of sampling inherent in other methods. Time measurement and signal processing does not exceed 0.2 s, which allows using this method in systems of automated process control. Measurement of the frequency of acoustic waves is performed with piezoelectric transducer and does not require sophisticated equipment.

The proposed method for controlling the progress of plasma chemical reactions regarding a change in the frequency of sound waves has been used to study the direct recovery of tungsten from tungsten hexafluoride under the influence of high-current electon beams (Vlasov, 2004). A good agreement with the data which were obtained by the weighing of a substrate placed in the reactor was obtained. An acoustic method to control the phase transition was also used for studying the synthesis of nanopowder oxides (Remnev, 2004d).

7. Measurement of energy absorbed by the gas in a closed reactor with exothermic reactions

The measurements show that for nitrogen and argon in a wide range of pressures (and therefore of beam energy input in a gas) a good correlation between the energy of sound vibrations and the electron beam energy input in a gas was obtained. This allows evaluating the energy input of a beam into gas using the amplitude of sound waves. The energy of sound waves is about 0.2% of the electron beam energy absorbed in the gas (Remnev et al., 2003a).

To measure the beam energy input into a gas, calorimetric measurements are commonly used. Here the energy of a pulsed power source is estimated by changes in temperature of a

calorimeter. The energy absorbed by the gas is obtained as the difference between the calorimeter readings and the known energy of the pulsed energy source. A disadvantage of this method is that some significant errors in measuring of the source energy which is absorbed by a high pressure take place. When the density of energy absorbed by the gas is more than 10 J/liter and at pressures above 400 Torr, the gas is heated to a temperature which is above that of the heating temperature of the calorimeter. The calorimeter is heated in this case not only by the influence of external energy, but also by the surrounding gas.

The energy of a pulsed electron beam absorbed by the gas in a closed reactor can be measured more precisely by a change in pressure (Moskalev and Sergeev, 1991). The electron beam energy absorbed by the gas is calculated as the product of the specific heat capacity of gas and the mass and the change in the gas temperature. The change of the gas temperature in the reactor is determined from the equation of state for an ideal gas due to a change of pressure in a closed reactor. A disadvantage of this method is that it is impossible to measure the electron beam energy absorbed by the gas in a closed reactor, in the case when an exothermic reaction takes place in the reactor. The change in pressure during the flow of exothermic reactions is due to the heating of the gas caused by absorption of the electron beam energy and heating because of the energy release in exothermic reactions.

In case of exothermic reactions in a closed reactor, the energy of a pulsed power source absorbed by a gas can be also measured by the amplitude of the standing sound waves. We have obtained that when a high-current electron beam with the following parameters: electron energy is 300–350 keV, beam current is 10–12 kA, pulse duration is 50–60 ns, is injected into a mixture of silicon tetrachloride with hydrogen, then a change of pressure in the reactor is 10–15 times bigger than changes due to heating of a gas by absorption of the electron beam energy. The dependence of the energy used for heating the gas in the reactor during the injection of an electron beam, on the gas mass is shown in Fig. 19. Curve 1 corresponds to the vapour-phase $SiCl_4$ or its mixture with argon and hydrogen (in this case m is the partial weight of silicon tetrachloride), curve 2, to that of argon and nitrogen. To prevent $SiCl_4$ condensation on the walls at pressures above 200 Torr (saturation vapour pressure at 30 ^oC) the reactor was heated to a temperature of 60 ^oC (the boiling point of $SiCl_4$ at normal conditions is 57 ^oC).

The dependence of the beam energy input on the gas mass for nitrogen and argon has an usual form: the growth at low pressures (200–600 Torr in the reactor is used for electrons with an energy of 300 keV), when the range of electrons in the beam and in the ionization cascade exceeds the length of the reactor. A part of the beam energy in this case is absorbed by the rear wall of the reactor. When the pressure is above 600 Torr (the mass is more than 0.08 mole) the electron beam is almost completely absorbed by the gas and in curve 2 a plateau is observed. The maximum energy used for gas heating and measured by the pressure jump is 70 J. The energy of the electron beam in a pulse is 90 J.

Calculation of the energy used for heating the silicon tetrachloride and its mixture with other gases during the electron beam injection (curve 1, Fig. 19), based on the indications of the pressure sensor showed that in this case, the release of energy exceeds by an order of magnitude the total energy of the beam and can not be explained only by the absorption of the electron beam in a gas. In addition, the dependence 1 in the investigated range of pressures (and the gas mass) is different than in curve 2 of Fig. 19, which also indicates another source of the heating of $SiCl_4$, beyond the heating by the electron beam. This can be explained by the occurrence in the reactor of the following exothermic reactions:

$$Cl + H_2 = HCl + H + 0.05\ eV$$

$$Cl + Cl + M = Cl_2 + M + 2.5\ eV$$

$$H + Cl_2 = HCl + Cl + 2\ eV$$

$$H + HCl = H_2 + Cl - 0.05\ eV$$

We have found that the frequency of standing sound waves generated in the 30 cm long reactor exceeds 100 Hz for the investigated gases. If the external effects of energy will exceed the period of these sound waves, the conditions for the formation of standing harmonic waves will be violated. Therefore, the duration of a pulsed energy source should be no more than 10^{-2} seconds.

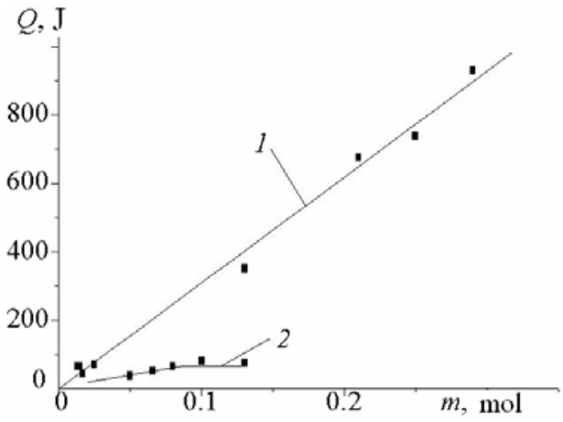

Fig. 19. The dependence of the energy used for heating the gas during the electron beam injection on the gas mass—$SiCl_4$ (1), argon, nitrogen—(2).

8. Registration of the conversion of gas-phase compounds in nanodispersed clusters by means of an increase in the absorption coefficient of sound waves

The presence in a gas of particles whose size is much larger than the gas molecules causes an increase in the attenuation of the sound waves propagating in the gas. The dependence of the absorption coefficient of energy of sound vibrations in the reactor on the pressure for different gases is shown in Fig. 20.

To compare the attenuation coefficients in the different plasma-chemical reactors (lengths 11.5 and 30 cm) and in different gases, the value of the attenuation coefficient was normalized by the coefficient *K*, calculated by the formula:

$$K = \sqrt{f_{sound}}\left(\frac{K_1}{r_0} + \frac{K_2}{l}\right) \quad ,$$

The points in Fig. 20 correspond to the experimental measurements, curve 1 is the calculation by (14). For nitrogen, argon and oxygen, the divergence between the calculated and experimental values of the absorption coefficient does not exceed 30%.

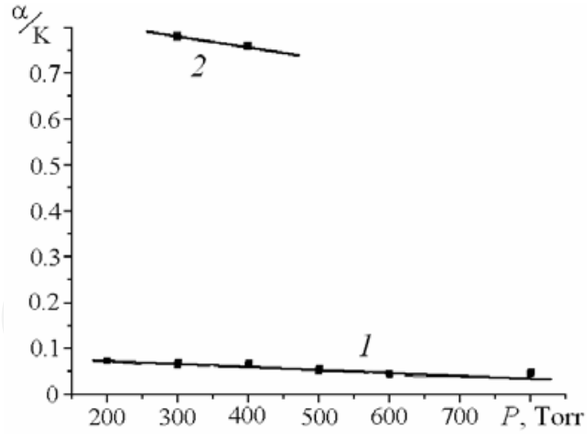

Fig. 20. The dependence of the normalized sound absorption coefficient on the pressure.

For the sound waves generated during the dissipation of a pulsed electron beam in the vapor-phase WF_6 (curve 2 in Fig. 20), the experimentally determined value of the absorption coefficient is much higher than (by a factor of 14–15) that calculated by (14). This can be explained by the formation of clusters in the reactor during the injection of the electron beam. The presence of large particles in the gas increases the absorption of sound waves. When the injection of a high-current electron beam in WF_6 occurs, a direct recovery of tungsten in the form of nanosized particles causes not only an increase in the frequency of the sound waves (Remnev et al., 2004c), but also a significant increase in the energy absorption of sound vibrations.

9. Acoustic diagnostics of a pulsed electron beam

When an electron beam passes through the target, it loses energy. The energy losses create a temperature field in the target. As a result, thermoelastic stresses appear and cause acoustic oscillations, whose shape corresponds to the distribution of electrons in the beam. This method allows of measuring the following parameters of a pulsed electron beam (Remnev et al., 2003b):

- Geometry of the electron beam
- Distribution of the energy over the beam cross-section
- The total energy of the beam
- Electron beam displacement across the plasma reactor

The experimental procedure consists in the following: directly in the beam arrival area a target-rod or a wire was placed. The target was placed perpendicularly towards the motion of the particles. A piezoelectric sensor was fixed at one end of the rod; and the other end has a conical shape to absorb the vibrations propagating in the opposite direction from the sensor. The piezoelectric transducer is clamped between the rod and cone, and the cone is also designed to absorb the vibrations passing through the sensor. The scheme of the detector is shown in Fig. 21.

As a target, a copper wire of rectangular cross-section of 2 mm × 5 mm was used. The wire was placed in a plasma-chemical reactor, being clamped between two rubber vacuum seals. A beam of electrons was directed through the foil of an exit window, the pressure in the reactor was atmospheric. After the beam interacts with the target, the waves propagate along the wire in both directions from the place where the electrons hit, they should be

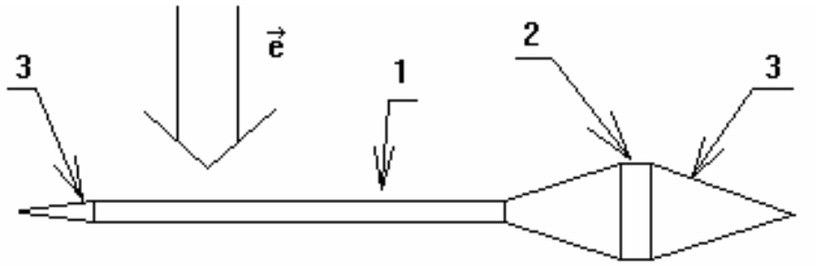

Fig. 21. The scheme of the acoustic diagnostics of the electron beam: 1-target, 2-piezoelectric sensor, 3-extinguishing cones.

diluted over time. This was achieved by increasing the length of the wires coming from opposite sides of the chamber. In order to eliminate the noise caused by an increase in the target potential when it is hit by the electrons, the wire was grounded.

9.1 Determination of the beam geometry

The duration of the first pulse of an acoustic signal, shown in Fig. 22, is determined by the diameter of the electron beam. Knowing the duration and sound velocity in a material of the absorber, the diameter of the beam cross-section can be determined.

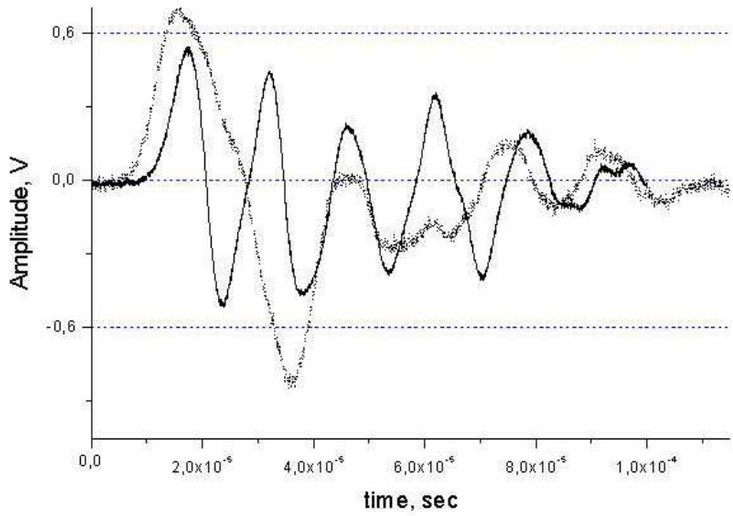

Fig. 22. Oscilloscope trace of the electrical pulses from the piezoelectric transducer when an electron beam is subjected to an absorber

We now determine the geometric dimensions of the beam. The length of the first pulse is 11 microseconds. Knowing the sound speed in the absorber, we obtain:

$$\Delta d = v_{sound} \cdot \Delta t = 3562 \cdot 10.96 \cdot 10^{-6} = 3.9\ cm$$

The diameter of the beam impress on a dosimetric film is 4 cm (see Fig. 4). Fig. 22 also shows an oscilloscope trace of a beam of reduced diameter. The change in the diameter was achieved by screening the absorber so that only the central part of the beam, with a diameter of 20 mm, hits the absorber. Therefore, knowing the duration of the first pulse, the diameter of the electron beam can be determined with a good accuracy.

9.2 Determination of the beam profile

Figure 23 shows the oscilloscope traces obtained at different beam profiles.

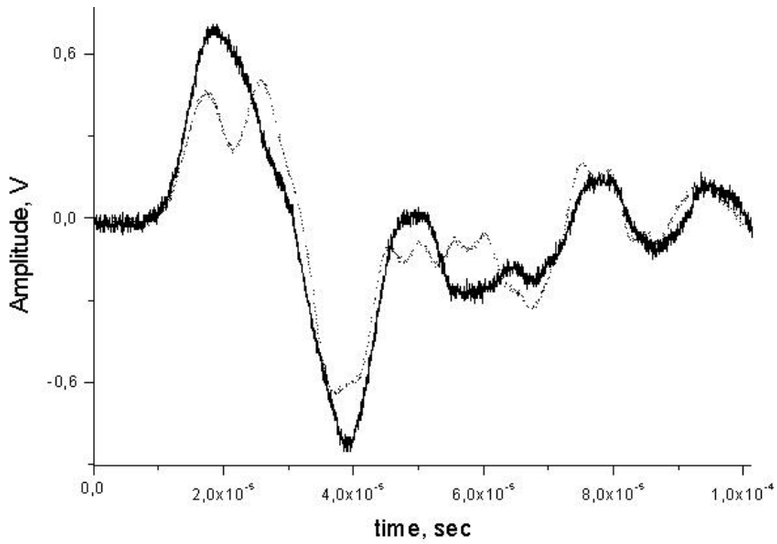

Fig. 23. Oscilloscope traces for different profiles of the beam

A change in the profile was achieved by shielding the central part of the absorber (see Figure 24), thus, the beam can be considered as hollow. The screen size was 10 mm.

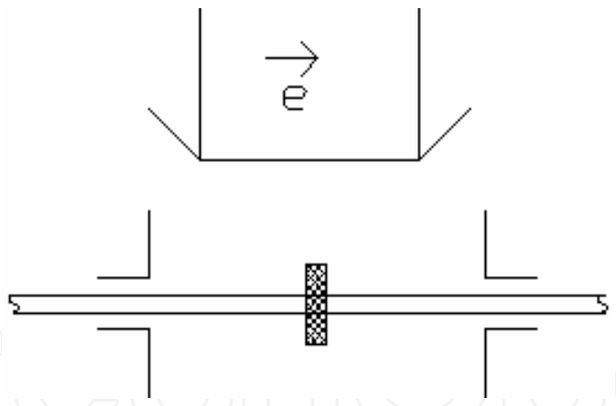

Fig. 24. Screening the center of the beam

A dip in the curve, due to a lack of a central part of the beam, is clearly visible in the graph.

9.3 Determination of the total energy of the beam

The measurements showed that the amplitude of the signal from the piezoelectric transducer is proportional to the total energy of the electron beam in a pulse. Figure 25 shows acoustic pulses for various values of the energy per pulse.

The beam energy was regulated by a grounded grid, which was located between the anode foil and the absorber. The dependence of the integral of the acoustic pulse on the total energy of the beam is shown in Figure 26. The presented dependence has a linear character, which allows a further use of the sensor as a probe of the total beam energy.

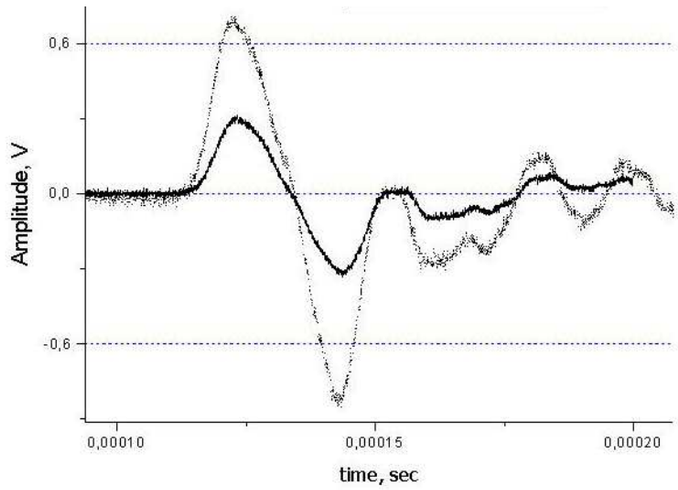

Fig. 25. Oscilloscope traces for different total energies of the beam.

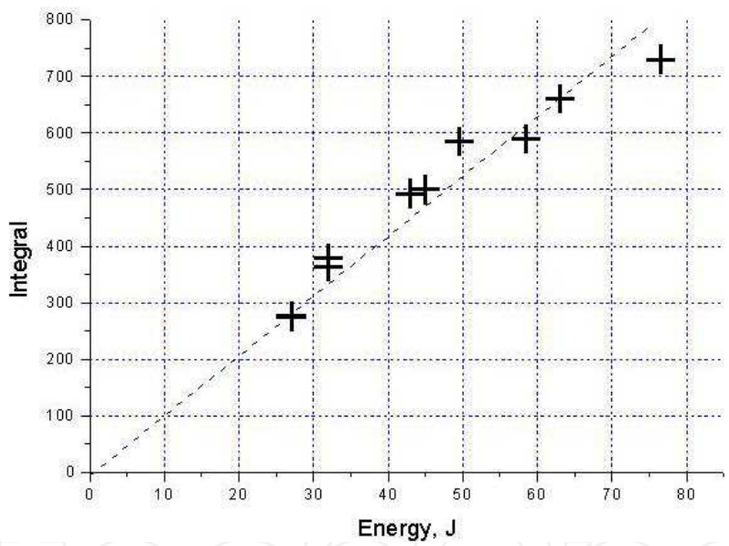

Fig. 26. The dependence of the integral of the acoustic pulse on the total electron beam energy

The advantages of radiation-acoustic diagnostic systems are the high noise immunity of the informative acoustic signal and the possibility of rapid analysis. The system can be used in any manufacturing plants or for research purposes without a significant change in the design of the accelerator chamber. The device is not exposed to the influence of a chemically active media, which makes it promising for the study of plasma chemical reactions initiated by a pulsed electron beam.

10. Conclusion

Our investigation of the sound waves generated in a closed reactor during the absorption of a pulsed electron beam shows that a simple experimental setup, recording the acoustic

vibrations can accurately control the plasma process, accompanied by a change in the phase composition of the initial reagent mixture. The formation of clusters in the volume of the reactor causes a change in the frequency of sound waves and a significant increase in the attenuation of the oscillations amplitude. Diagnostics regarding the sound waves in the reactor can be used for operational control of the plasma process. When reducing the diameter of the reactor, the resonance frequency of transverse acoustic waves increases and the accuracy of measurement of methane conversion increases as well.

11. References

Bondar, Y.F., Zavorotny, S.I., Ipatov, A.L., Mkheidze, G.I., Ovchinnikov, A.A., Savin, A.A. (1982) The study of a relativistic electron beam transport of in a dense gas. Plasma Physics, 8(6): pp. 1192–1198.

Isakovich, M.A. (1973) General acoustics. Moscow: Nauka.

Konstantinov, B.P. (1974) A hydrodynamic sound formation and propagation of the sound in the suspension of microparticles in a gas. Moscow: Nauka.

Lyamshev, L.M. (1996) Radiation acoustics. Moscow: Fizmatlit-Nauka.

Molevich N.E., Nenashev, V.E. (2000) Influence of the volume viscosity on the sound propagation in the suspension of microparticles in a gas. Acoustical Physics,4: pp. 520–525.

Moskalev, V.A., Sergeev, G.I. (1991) The measurement of charged particle beams. Moscow: Energoatomizdat.

Pushkarev, A.I., Pushkarev, M.A., Zhukov, L.L., Suslov, A.I. (2001) Measurement of the energy dissipation of the electron beam in a dense gas by a quick-response differential pressure sensor. Physics, 7: pp. 93–97.

Pushkarev A.I., Pushkarev M.A., Remnev, G.E. (2002) Sound waves generated due to the absorption of a pulsed electron beam in gas. Acoustical Physics, 48(2) pp. 220–224.

Pushkarev, A.I., Novoselov, Y.N., Remnev, G.E. (2006) Chain processes in a low-temperature plasma. Novosibirsk: Nauka.

Pushkarev, A.I. and Sazonov, R.V. (2008) Acoustic method of monitoring the conversion of methane into carbon. Acoustical Physics, 54(1): pp. 135–137.

Remnev, G.E., Pushkarev, A.I., Pushkarev, M.A., Krasilnikov, V.A., Guzeeva, T.I. (2001) Monitoring of the changes in chemical composition of gases in a plasma chemical reactor during condensation of the reaction products using the acoustic-wave frequency data. Russian Physics Journal 44(5): pp. 482-485.

Remnev, G.E., Pushkarev, A.I., Pushkarev, M.A. (2003a) Method of monitoring the changes in the phase composition of a gas mixture in a closed reactor Patent of Russia № 2215799 RF, MPK7 S22V 5 /00. / Applied 04.03.2002. Published. 10.11., Bul. № 31.

Remnev, G.E., Pushkarev, A.I., Ezhov, V.V. (2003b) Radiation-acoustic diagnostic of the profile of a pulsed electron beam. Proceedings of the 11th International Scientific School-Seminar "Physics of the pulsed discharges in condensed media". Nikolaev, August 2003, pp. 77–78.

Remnev, G.E., Furman, E.G., Pushkarev, A.I., Kondratiev, N.A., Goncharov, D.V. (2004a) High-current pulsed accelerator with matched transformer: construction and exploitation characteristics. IEEE Transactions on fundamentals and materials, 124(6): pp. 491–495.

Remnev G.E., Furman E.G., Pushkarev A.I., Karpuzov S.B., Kondrat'ev N.A., and Goncharov D.V. (2004b) A High-Current Pulsed Accelerator with a Matching Transformer // Instruments and Experimental Techniques, , v. 47, №3, p. 394–398.

Remnev, G.E., Pushkarev, A.I., Pushkarev, M.A., Krasilnikov, V.A., Guzeeva, T.I. (2004c) Method of a direct reduction of halides Patent of Russia № 2228239. /. Applied 04.02.2002, published 10.05., Bul. № 13.

Remnev, G.E., and Pushkarev, A.I. (2004d) Research of chain plasmochemical synthesis of superdispersed silicon dioxide by pulse electron beam. IEEE Transactions on fundamentals and materials, 124(6): pp. 483–486.

Vlasov, V.A., Pushkarev, A.I., Remnev, G.E. (2004e) Experimental study and mathematical modelling of the recovery processes of fluoride compounds by a pulsed electron beam. Proceedings of Tomsk Polytechnic University, 307(5): pp. 89–93.

Yaworski, B.M., Detlaf, A.A. (1968) Handbook of physics. Moscow: Nauka.

Zhivotov, V.K., Rusanov, V.D., Fridman A.A. (1985) Diagnostics of non-equilibrium chemically active plasma. Moscow: Energoatomizdat.

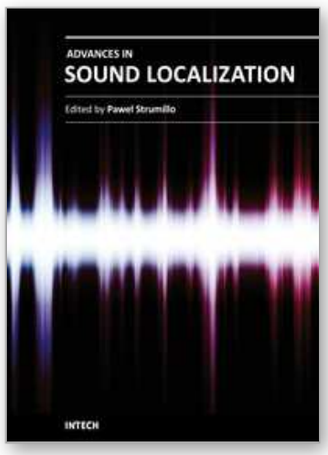

Advances in Sound Localization
Edited by Dr. Pawel Strumillo

ISBN 978-953-307-224-1
Hard cover, 590 pages
Publisher InTech
Published online 11, April, 2011
Published in print edition April, 2011

Sound source localization is an important research field that has attracted researchers' efforts from many technical and biomedical sciences. Sound source localization (SSL) is defined as the determination of the direction from a receiver, but also includes the distance from it. Because of the wave nature of sound propagation, phenomena such as refraction, diffraction, diffusion, reflection, reverberation and interference occur. The wide spectrum of sound frequencies that range from infrasounds through acoustic sounds to ultrasounds, also introduces difficulties, as different spectrum components have different penetration properties through the medium. Consequently, SSL is a complex computation problem and development of robust sound localization techniques calls for different approaches, including multisensor schemes, null-steering beamforming and time-difference arrival techniques. The book offers a rich source of valuable material on advances on SSL techniques and their applications that should appeal to researches representing diverse engineering and scientific disciplines.

How to reference
In order to correctly reference this scholarly work, feel free to copy and paste the following:

A. Pushkarev, J. Isakova, G. Kholodnaya and R. Sazonov (2011). Sound Waves Generated Due to the Absorption of a Pulsed Electron Beam, Advances in Sound Localization, Dr. Pawel Strumillo (Ed.), ISBN: 978-953-307-224-1, InTech, Available from: http://www.intechopen.com/books/advances-in-sound-localization/sound-waves-generated-due-to-the-absorption-of-a-pulsed-electron-beam

INTECH
open science | open minds

InTech Europe
University Campus STeP Ri
Slavka Krautzeka 83/A
51000 Rijeka, Croatia
Phone: +385 (51) 770 447
Fax: +385 (51) 686 166
www.intechopen.com

InTech China
Unit 405, Office Block, Hotel Equatorial Shanghai
No.65, Yan An Road (West), Shanghai, 200040, China
中国上海市延安西路65号上海国际贵都大饭店办公楼405单元
Phone: +86-21-62489820
Fax: +86-21-62489821

IntechOpen